Received: 6 September 2023 | Revised: 7 January 2024 | Accepted: 11 February 2024

DOI: 10.1002/app.55340

RESEARCH ARTICLE

Applied Polymer SCIENCE WILEY

Robust poly(p-phenylene oxide) anion exchange membranes reinforced with pore-filling technique for water electrolysis

Zhiming Feng[1] | **Gaurav Gupta**[2] | **Mohamed Mamlouk**[3]

[1]Chemical Engineering, Imperial College London, London, UK

[2]Chemical Engineering, Lancaster University, Lancaster, UK

[3]School of Engineering, Newcastle University, Newcastle upon Tyne, UK

Correspondence
Zhiming Feng, Chemical Engineering, Imperial College London, London SW7 2BX, UK.
Email: z.feng@ic.ac.uk

Funding information
Engineering and Physical Sciences Research Council, Grant/Award Number: EP/T00939X/1

Abstract

Mechanical robustness and durability are crucial for anion exchange membranes to guarantee the longevity and consistent performance of AEM water electrolysis (AEMWE) systems. In this study, a composite membrane based on the quaternized poly(p-phenylene oxide) (QPPO)/polytetrafluoroethylene (PTFE) was developed. This membrane was fabricated by enhancing the QPPO-based AEM through a pore-filling technique within a porous PTFE structure. The tensile strength of the composite membrane was increased significantly from 16.5 to 31 MPa. The conductivity of the composite membrane was 6.25 $mScm^{-1}$ lower than 30 $mScm^{-1}$ of the QPPO-based membrane at 20°C, resulting from the low volume fraction of QPPO in the composite membrane. At 40% RH, the net change mass of the composite membrane is 1.59%, much lower than that of QPPO-based membrane (10.98%) at 40°C. The composite membrane demonstrated a significantly increased lifetime in the working electrolyzer (>200 h) compared with an otherwise identical electrolyzer assembled with a QPPO-based membrane (50 h).

KEYWORDS

electrochemistry, mechanical properties, synthesis and processing techniques, water electrolysis

1 | INTRODUCTION

Anion exchange membranes (AEMs) play a crucial role in water electrolysis, working as the barrier between evolved oxygen and hydrogen gases to avoid their direct mixing and provide an ionic conduction path to transport OH^- from cathode to anode.[1–4] However, standalone membranes have limitations, as they are subjected to harsh operational environments characterized by elevated temperatures, substantial external forces, and significant levels of oxidation/reduction species.[5] Over time, the demanding conditions can lead to the degradation of the AEM, which can reduce its performance and lifespan.[6–8] Therefore, modification strategies to AEMs were taken into consideration to meet these requirements.[9] One of the promising methods is to prepare composite membrane structures, such as sandwich and pore-filled structures.[10–12] These membranes have showcased exceptional ion conductivity, robust alkaline stability, and enhanced mechanical properties, rendering them optimal for water electrolysis. Composite membranes can be categorized into organic, inorganic, and

hybrid enhancements based on the introduced substances. Inorganic composite membranes usually consist of ceramics, metals, or metal oxides, offering superior chemical and thermal stability compared with organic materials.[13–16] Additionally, they are less prone to fouling or degradation, making them well-suited for demanding operating conditions. However, manufacturing inorganic membranes can be more costly and challenging than organic materials.[17,18] The organic composite membrane can be less expensive and offer improved performance. Polyethylene (PE) is a commonly used substrate due to its porous structure and good chemical resistance.[19,20] Wang and coworkers reinforced poly(fluorenyl-co-terphenyl piperidinium)-based AEM using high-density PE. They used EtOH as an assistant cosolvent to enhance the penetration efficiency of the polymer solution. The tensile strength of the composite membrane was higher than 120 MPa.[21] Apart from PE, Hwang and coworkers used porous (PTFE) as the substrate in proton exchange membrane fuel cells. The reinforced membrane achieved long-lasting single-cell operation for 21,000 wet/dry cycles.[22] Zhang and coworkers focus on the fabrication and application of a novel PTFE-based composite anion exchange membrane (AEM) in direct hydrazine hydrate fuel cells (DHFC). The membrane, prepared through in situ thermal polymerization and quaternary amination, exhibits high hydroxide conductivity and achieves a promising DHFC power density, making it a potential candidate for AEMFC applications.[23] Zhao and coworkers present a low-toxic and facile method for preparing a novel PTFE-based composite AEM for alkaline fuel cells. The membranes are synthesized through in situ polymerization and subsequent hydrolysis and quaternary amination, resulting in high ionic exchange capacity, excellent mechanical and chemical stability, and promising performance in alkaline fuel cells. The synthesis method avoids the use of carcinogenic chemicals and has been characterized through various techniques, demonstrating the suitability of these membranes for alkaline fuel cell applications.[24]

Poly(2,6-dimethyl-1,4-phenylene oxide) (PPO) is a commercially available polymer soluble in various organic solvents and can be readily modified for further functionalization. Although its stability is somewhat lower than that of aryl-ether-free polymers, PPO still has better chemical stability than engineering polymers such as poly(ether sulfone)s or poly(ether ketone)s are commonly used in AEMs.[25,26] As a result, PPO has been extensively employed as a material for AEMs because of its exceptional thermomechanical stability and the benefits mentioned above.[25,27,28]

In this research, the highly conductive quaternized PPO-based AEM was reinforced by using the PTFE substrate. The physical and electrochemical properties of PTFE-reinforced AEMs were investigated to elucidate the advantages of the composite membrane. The composite membrane exhibited notably improved mechanical strength and durability compared with the standalone PPO-based membrane.

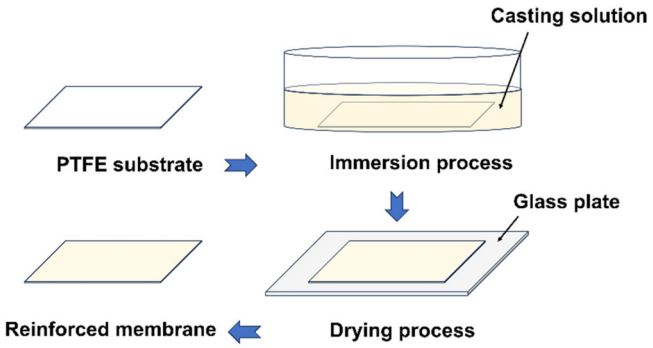

SCHEME 1 The manufacturing processes. [Color figure can be viewed at wileyonlinelibrary.com]

2 | EXPERIMENTAL

2.1 | Materials

As synthesized chloromethylated poly(p-phenylene oxide) (PPO, product number 181781, white power), potassium hydroxide (KOH), trimethylamine (TMA, 45 wt%), tetrahydrofuran (THF) were purchased from Sigma-Aldrich and used without further purification. PTFE (pore size 0.5 μm) was purchased from Toyo Roshi Kaisha, Ltd, Japan. Pt/C catalyst was purchased from fuel cell store (Product Code: 591478).

2.2 | The preparation of the QPPO/PTFE composite membrane

Scheme 1 shows the manufacturing processes of quaternized poly(p-phenylene oxide) (QPPO)/PTFE based composite membrane. A 0.5 g chloromethylated PPO (ClPPO) was dissolved in THF to prepare the casting solution (14 wt %). The PTFE porous membrane (pore size 0.5 μm) was immersed into the impregnation solution under ultrasonic vibration for 2 min to ensure the even distribution of the solution in the pores of the PTFE membrane substrate. The ultrasonication of the membrane was carried out using a Fisher Scientific FB15049 ultrasonicator at room temperature. The vibration power of the device was 95 W. The ClPPO/PTFE based membrane was quaternized by immersed separately in TMA, KOH, and deionized water

to obtain the QPPO/PTFE based composite membrane.[29,30] The concentration of TMA (trimethylamine) used was 45%. The concentration of KOH utilized in our experiments was 1 M. The membrane was dried using an air-drying method over night at room temperature.

2.3 | Mechanical properties

The mechanical properties of the samples were measured using a universal testing machine (Model-Tinius Olsen H25KS, Tinius Olsen, USA) to obtain the stress–strain plot. The samples were cut into a dog-bone configuration, featuring an effective area measuring 5 mm × 10 mm. The tensile strength and elongation at the point of fracture were assessed under standard atmospheric conditions, utilizing a stretching rate of 2 mm min^{-1}.

2.4 | Dynamic gravimetric vapor sorption

Dynamic gravimetric vapor sorption (DVS) can determine materials' vapor sorption isotherms. Hidden Isochena (advancing sorption analysis) was used for those studies to measure the weight change as the function of time at target relative humidity. An ultramicro balance is used to measure the uptake and loss of vapor gravimetrically. The instrument with high mass resolution and baseline stability can identify the adsorption and desorption of tiny amounts of probe molecules. QPPO and QPPO/PTFE-based membranes were tested. The dry membranes' weight was 17.12 and 14.12 mg, respectively.

2.5 | Ionic conductivity and activation energy

The membrane through-plane conductivity was measured using an in-house test cell with an electrode area of 1.77 cm^2. To avoid direct reaction with the CO_2 in the air, the membrane was kept submerged in deionized water while loaded in a conductivity cell and was tested under an N_2 atmosphere. The membrane was sandwiched between two gas diffusion layer carbon electrodes in the cell, with 100% relative humidity and elevated temperature, verified by temperature and humidity sensors, respectively. The ionic conductivity was calculated by using Equation 1.

$$\sigma = \frac{4L}{R(\pi d^2)}, \quad (1)$$

where σ is the hydroxide ionic conductivity, L is the membrane thickness, R is the resistance derived from the impedance value at a zero-phase angle, and d is the diameter of the actual testing area. The impedance was measured using the same procedure previously reported.[31]

2.6 | Single cell test

$NiCo_2O_4$ was synthesized through a thermal decomposition process following our previous reported procedures.[30] $Ni(NO_3)_2{\cdot}6H_2O$ (14.54 g) and $Co(NO_3)_2{\cdot}6H_2O$ (29.1 g) were dissolved in 100 mL of methanol and then heated at 338 K to facilitate the removal of the solvent. The dried powder sample was subsequently subjected to calcination at 648 K for a period of 20 h, followed by an additional 12 h of ball milling. The electrochemical performance of the membrane and the ionomer were tested in electrolyzer cells by preparing a membrane electrolyte assembly using Pt/C catalyst at the cathode (0.4 mg cm^{-2}) and $NiCo_2O_4$ at the anode (2 mg cm^{-2}).[30] At the anode side, titanium fiber felt gas diffusion layer (GDL) with a thickness of 0.3 mm and 78% porosity (Bekaert Toko metal fiber Co., Ltd.) was used for the oxygen evolution reaction. The anode catalyst ink, consisting of $NiCo_2O_4$, 28 wt% ionomers and *N*-methylpiperidine solvent, was sprayed on the titanium GDL directly. As for the hydrogen evolution reaction, the electrode was used for non-wet-proofed carbon GDL with micro porous layer (product code H2315 C9, Freudenberg Germany). The catalyst at the cathode was 20% Pt/C, 28 wt% ionomers and isopropanol. Besides, the QPPO/PTFE composite membrane was also tested for electrochemical performance with QPPO as the ionomer. The electrochemical measurement, including cyclic voltammetry (CV), electrochemical impedance spectroscopy (EIS) and potentiostatic durability test, were made using the Autolab potentiostats instrument (PGSTAT302 N). The two-electrode method was used for single cell test. The working electrode is connected with the anode while the counter electrode was connected with the cathode. The experiments were operated by circulating 0.1 M NaOH supporting electrolyte to both anode and cathode. The working area is 1 cm^2. CV was studied by cycling between 1.3 to 2 V at a scan rate of 1 mV s^{-1}. EIS was measured at 1.7 V at 40°C. For the durability test of the electrolyzer, the voltage was set to 1.7 V at 40°C.

3 | RESULTS AND DISCUSSION

3.1 | QPPO/PTFE composite membrane

Polytetrafluoroethylene (PTFE, thickness 70 μm, 68% porosity, pore size 0.5 μm) was utilized as the matrix in

this study to reinforce the QPPO-based membrane. The ClPPO was homemade following the papers.[29,30] As is shown in Table 1, the weight of PTFE increased from 98 to 113 mg, and the thickness increased from 70 to 76 μm after immersion in impregnation solution and drying off the solvent. The density of the Cl-PPO is ca. 1.1 gcm^{-3}. The area of PTFE is 6.5 cm^2.

This means there is a total of ca. 6 μm layer of ClPPO covering the PTFE membrane surface divided between the two faces of the PTFE membrane. This layer is not homogeneously covering the entire PTFE surface, as shown in Figure 1e,f where some of the PTFE pores in some sections of the membrane remain visible. The remaining ClPPO also partially fill the available pores in the PTFE. Upon the fabrication of the composite membrane, ClPPO adheres to the surface of PTFE and permeates its porous structure. This study posits a uniform distribution of ClPPO within the entire system. Our methodology involves a two-step quantitative analysis: initially, we ascertain the mass of ClPPO adhered to the PTFE surface; subsequently, we evaluate the mass of ClPPO occupying the PTFE pores, leading to the determination of the volume occupied by ClPPO and the computation of the pore filling ratio.

In detail, the observed increment in the thickness of the composite membrane, as compared with the unmodified PTFE matrix, is attributed to the ClPPO adhesion. The thickness augmentation is quantified at 6 μm. Given the known surface area of PTFE (6.5 cm^2) and the density of ClPPO (1.1 g/cm^2), the mass of ClPPO adhering to the PTFE surface is calculated to be approximately 4.29 g. Furthermore, the total mass increment of the composite membrane is recorded at 15 mg, implying the aggregate mass of ClPPO to be 15 mg. This allows for the deduction that ClPPO filling the PTFE pores amounts to 10.71 mg, occupying a volume of 9.736×10^{-3} cm^3. Through volumetric analysis, the total volume of PTFE is calculated to be 0.0455 cm^3, with an inherent porosity of 68%. Consequently, the pore volume is calculated as 0.03094 cm^3. Thus, it is inferred that ClPPO occupies approximately 31.4% of the PTFE pore volume, highlighting a significant degree of pore infiltration by the ClPPO in the composite structure. This means the volume fraction of ClPPO in the composite membrane is around 21.4%. Tortuosity describes the sinuosity of the pore space and influences flux transport in porous media.[32,33] In porous membranes, high tortuosity normally reflects a long transport path. The tortuosity factor can be obtained via the reciprocal of porosity, 1.5 in this case.[34–36] For the composite membrane, the composite membrane's anticipated conductivity compared with that of homogenous QPPO-based AEM would be a factor of 0.1 ($0.21^{1.5}$), which can be obtained from the porosity to the power of tortuosity.[33,37,38]

TABLE 1 Parameter of PTFE and QPPO/PTFE composite membrane.

	PTFE	QPPO/PTFE composite membrane
Weight (mg)	98	113
Thickness (μm)	70	76

Abbreviation: QPPO, quaternized poly(p-phenylene oxide).

The pure PTFE is hydrophobic, while the PPO/PTFE composite membrane becomes hydrophilic due to the high hydrophobic property of PPO. As is shown in Figure 1, the fibers of PTFE are apparent and separated from each other. The threads seem to congregate together upon ClPPO impregnation, where ClPPO acts as the binder. The PTFE is the continuous phase, and the ClPPO is the disperse phase.

3.2 | Mechanical properties

The mechanical property of the QPPO/PTFE composite membrane was tested and compared with pristine QPPO and porous PTFE membranes. As is shown in Figure 2, the tensile strength of QPPO/PTFE-based composite membranes was significantly higher than that of homogenous QPPO. Tensile strength increased from 16.5 ± 2.5 MPa (14 MPa for QPPO-1 and 19 MPa for QPPO-2 to 31 ± 2 MPa) (29 MPa for QPPO/PTFE-1 and 33 MPa QPPO/PTFE-2). The pristine porous PTFE-based membrane showed excellent mechanical strength and good elongation at a break of 43 MPa and 60%, respectively. The pristine PTFE membrane is hydrophobic, and the PTFE membrane used to test mechanical properties was dry. For the QPPO/PTFE composite membrane, the membrane becomes hydrophilic in the presence of QPPO. The water inside the composite membrane among PTFE fiber chains can act as lubricants, improving membrane flexibility but reducing tensile strength from that of PTFE of 43 to 31 ± 2 MPa for composite membrane. Good flexibility keeps the membrane from breaking under mechanical stresses, especially in the presence of electrolyzer clamping force. The addition of PTFE to QPPO can potentially influence the tensile strength of the composite membrane from those aspects. PTFE is known for its high tensile strength and mechanical properties. When added to QPPO, it can act as a reinforcing agent, enhancing the overall tensile strength of the composite membrane. The presence of PTFE can improve the load-bearing capacity and resistance to deformation under stress. Besides, the amount or concentration of PTFE in the composite membrane can affect its tensile

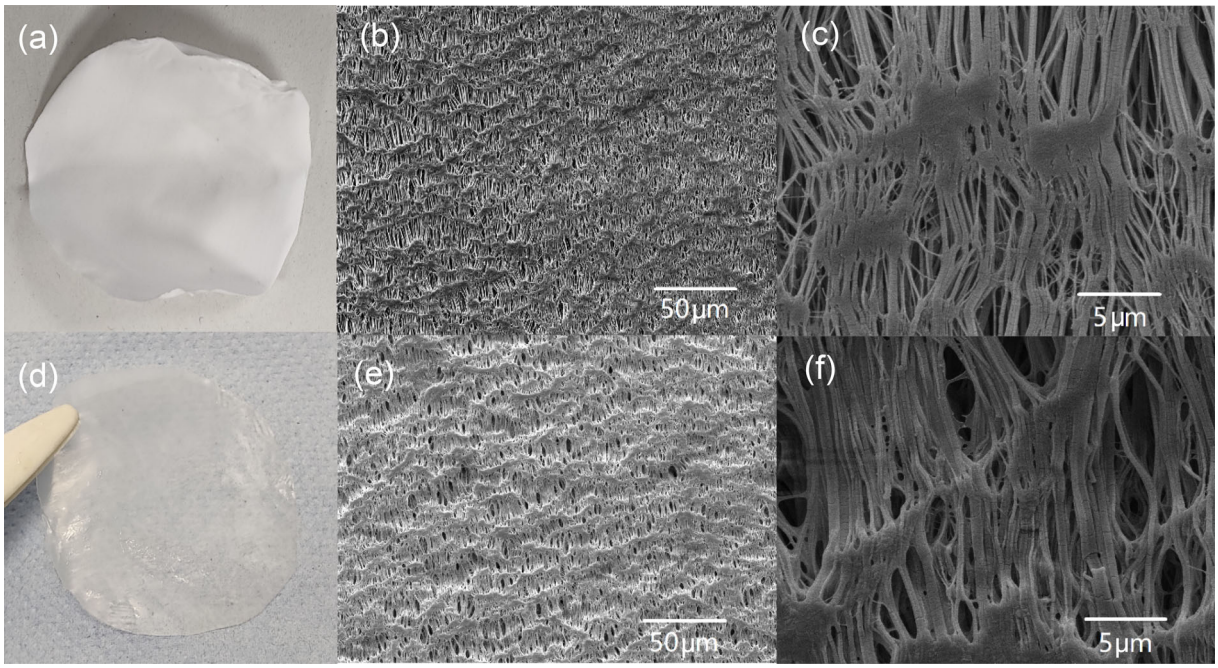

FIGURE 1 (a) Unfilled porous polytetrafluoroethylene (PTFE) and the corresponding SEM surface morphology of pure PTFE membrane (b) 1k×, (c)10k×. (d) The chloromethylated PPO (ClPPO) impregnated PTFE membrane and the SEM surface morphology of pure PTFE membrane (e)1k×, and (f)10k×. [Color figure can be viewed at wileyonlinelibrary.com]

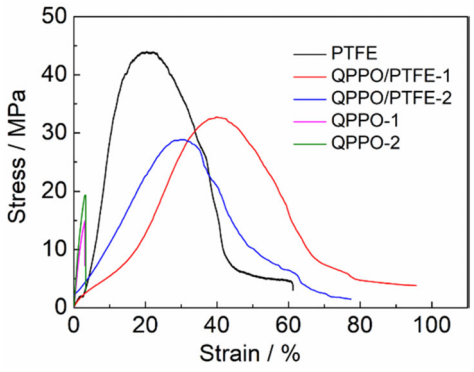

FIGURE 2 Mechanical properties of quaternized poly(p-phenylene oxide) (QPPO)-based membrane (wet), PTFE (dry), and QPPO/PTFE (wet) based membranes as dry samples. [Color figure can be viewed at wileyonlinelibrary.com]

strength. Generally, an increase in the PTFE content leads to an increase in the tensile strength up to a certain point. However, an excessive amount of filler may lead to agglomeration, reduced polymer matrix integrity, or weaker interfacial bonding, which can negatively impact the tensile strength. In addition, processing conditions: The processing method used to fabricate the composite membrane can influence its tensile strength. Factors such as temperature, pressure, and mixing time during the blending or compounding process can affect the dispersion and alignment of PTFE within the QPPO matrix, thereby affecting the overall tensile strength. In addition, the compatibility between PTFE and QPPO is crucial. Proper dispersion and adhesion of the QPPO within the PTFE matrix are necessary for the transfer of stress between the components. A good interfacial interaction between PTFE and QPPO can contribute to improved tensile strength. Besides, the increased final strain response of the QPPO/PTFE composite (87% ± 9%) compared with PTFE alone (60%) can be attributed to the combined effects of QPPO and PTFE in the composite system. The inclusion of PTFE in the composite introduces certain beneficial aspects that enhance the mechanical properties beyond what is observed with PTFE alone. One possible explanation is that PTFE, being a highly flexible and deformable polymer, provides a certain level of elasticity and compliance to the composite membrane. This allows the QPPO/PTFE composite to withstand larger strains before failure compared with PTFE alone, which exhibits a lower final strain response. The presence of PTFE can enhance the composite's ability to accommodate strain and deformation without experiencing significant structural damage. Additionally, the interaction between QPPO and PTFE can lead to a synergistic effect on the mechanical properties of the composite. QPPO may act as a reinforcing component, improving the overall strength and stability of the composite structure. This reinforcement can contribute to the composite's ability to sustain higher strain levels without

failure. It is important to note that the specific mechanisms and interactions between QPPO and PTFE, as well as their contributions to the composite's mechanical properties, may involve complex molecular and interfacial phenomena.

The enhancement of tensile strength over pristine QPPO should result in more extended durability under mechanical stresses and, consequently, a longer lifetime of the electrolyzer.

3.3 | Ionic conductivity

The ionic conductivity of the composite membrane was tested from 20 to 80°C under an N_2 atmosphere. As shown in Figure 3, the conductivity of the QPPO/PFTE composite membrane is, as expected, lower than the QPPO-based membrane. At 20°C, the conductivity of the QPPO/PTFE-based membrane is 6.25 $mScm^{-1}$, much lower than 58.30 $mScm^{-1}$ of QPPO based membrane. That means the conductivity of composite membranes is only 11% of that of pristine QPPO. The expected conductivity considering the impregnated volume fraction of QPPO and PTFE tortuosity is significantly higher at 28%. The additional loss of conductivity can be attributed to lower water uptake. Impregnation of QPPO in PTFE pores will restrict QPPO swelling. Due to the hydrophobic nature of PTFE repelling water away, membrane water uptake will be limited further. A lack of conductivity increase can be evidence of this due to lower water uptake or dehydration in the composite membrane at temperatures above 50°C. In contrast, steady growth is still seen for pristine QPPO membranes up to 80°C. This will be further studied in the following section.

3.4 | Dynamic gravimetric vapor sorption

Water sorption is used to characterize the adsorption ability of AEM towards water molecules. Adsorption isotherm models can depict the interaction mechanisms between the adsorbent and the adsorbate at a constant temperature based on the test's equilibrium data and the adsorbent's adsorption properties.[39] Dynamic gravimetric vapor sorption (DVS) was tested to study the water sorption and diffusion coefficient.

The experimental sorption data for QPPO and QPPO/PTFE-based membranes are shown in Figure 4b,c. Weight change and relative humidity were obtained as the function of time. The membrane was dried and absorbed the water vapor under relative humidity. QPPO membrane absorbed water to reach a saturation level

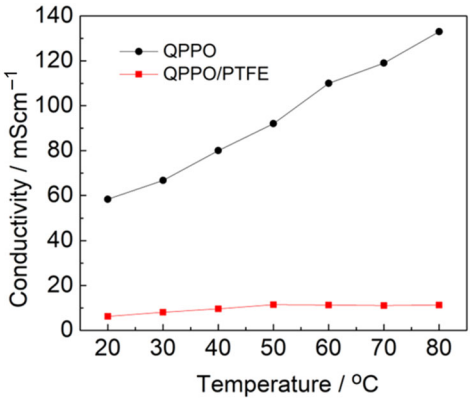

FIGURE 3 Ion conductivity of quaternized poly(p-phenylene oxide) (QPPO) and QPPO/PTFE. [Color figure can be viewed at wileyonlinelibrary.com]

faster (54 min) than QPPO/PTFE composite membrane (72 min) despite the higher level of water uptake in pristine QPPO AEM. This means water diffusion is faster (larger diffusion coefficient) in QPPO than QPPO/PTFE. This can be explained by the inhomogeneous composition of QPPO/PTFE, where larger hydrophilic regions were larger water clusters (slower to diffuse), and hydrophobic regions (PTFE).

To illustrate the water uptake equilibrium more clearly, the water vapor sorption isotherm data (the equilibrium water content C_w) were plotted against the target RH in Figure 4a. QPPO-based membrane has higher water sorption/uptake than QPPO/PTFE composite membranes. At 40% RH, the net change mass is 10.98%, while for the composite membrane, that is 1.59%. The QPPO and QPPO/PTFE-based membrane sorption isotherm exhibited a concurrent mass change value increase with the target RH increase. Similarly, at 90% RH, water uptake of QPPO was 28%, while for QPPO-PTFE, it was only 5.3%. It is worth pointing out that water uptake of PPO/PTFE of 5.3% at 90% RH can increase to 40% if the data are normalized by the 13wt% of QPPO in QPPO/PTFE. This assumes water is only trapped or absorbed by PPO. However, the reality is that water can also fill the unfilled pores of PTFE through capillary action. As discussed above, 31.4% of the PTFE pores or 29% of the total membrane volume, remain unfilled. Considering a density of 1 g cm^{-3} for the polymer and water, this means that a significant fraction of the 13% water sorbed can be caused by trapped water in unfilled PTFE pores, which doesn't contribute to conductivity.

According to the categorization of isotherm characteristics,[39] QPPO and QPPO/PTFE composite membranes show the Type II isotherms (concave upward) curve, which typically describes adsorption on mesoporous monolayer materials (usually disperse solids

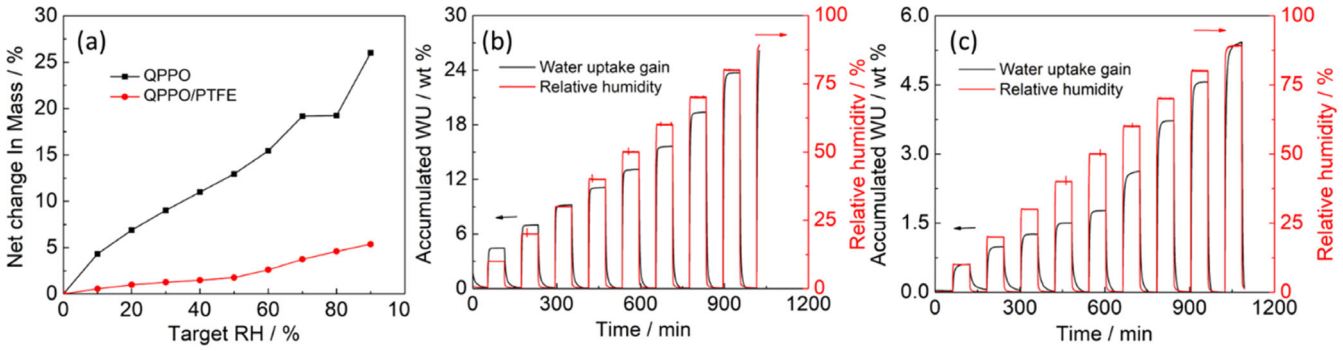

FIGURE 4 (a) Water vapor sorption isotherms of quaternized poly(p-phenylene oxide) (QPPO) and QPPO-PTFE based membranes at 60°C. Experimental sorption data (weight change and relative humidity change) of QPPO (b) and QPPO/PTFE (c) based membrane at 60°C. [Color figure can be viewed at wileyonlinelibrary.com]

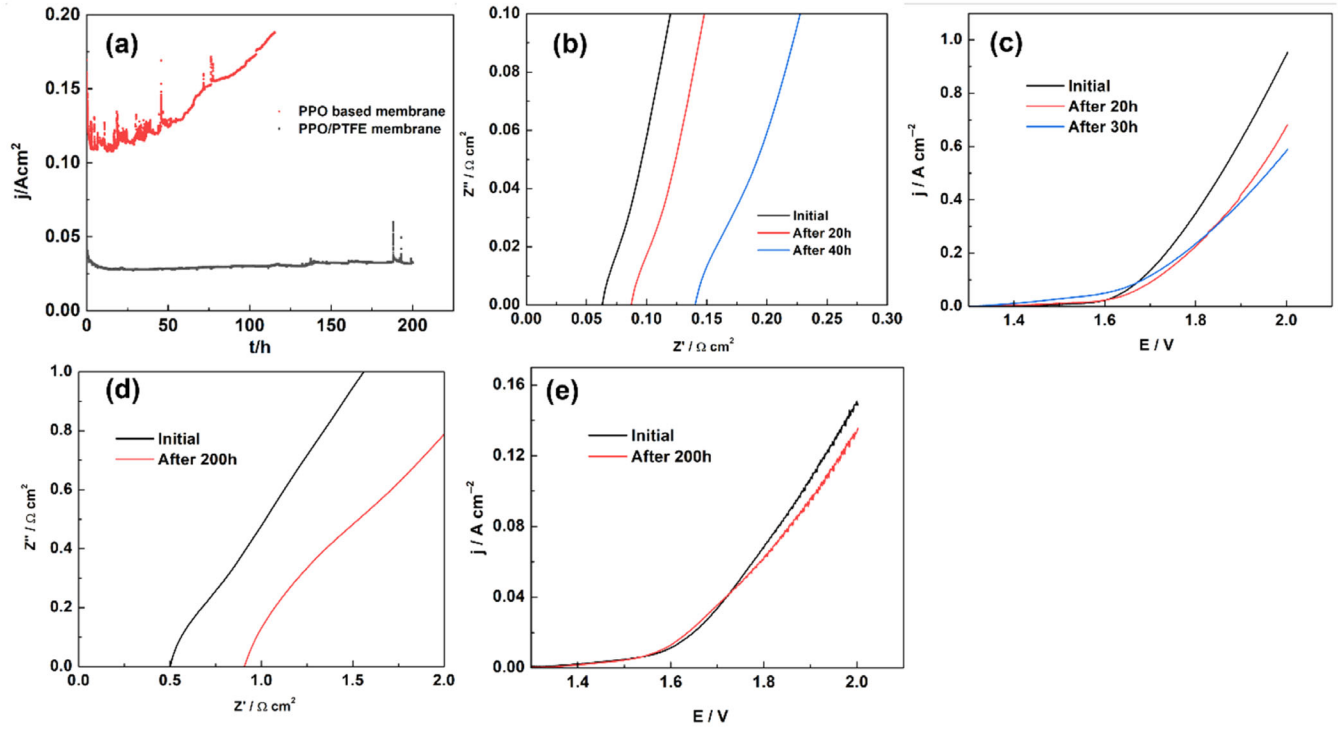

FIGURE 5 (a) Comparison of long-term tests of quaternized poly(p-phenylene oxide) (QPPO)-based membrane and QPPO/PTFE membrane at 1.7 V in 0.1 NaOH at 40°C. (b) Electrochemical impedance spectroscopy (EIS) of QPPO-based membrane before and after the long-term test. (c) Polarization curves of poly(2,6-dimethyl-1,4-phenylene oxide) (PPO)-based membrane before and after the long-term test. (d) EIS of QPPO/PTFE composite membrane before and after the long-term test. (e) Polarization curves of QPPO/PTFE based membrane before and after long-term. [Color figure can be viewed at wileyonlinelibrary.com]

with >50 nm pore diameter) at low pressure and on mesoporous multilayer material at high pressure near saturation with no hysteresis.

3.5 | Single cell test

Figure 5a shows the long-term durability test of the QPPO-based AEM and the QPPO/PTFE composite AEM assembled in the cell at 1.7 V in 0.1 NaOH at 40°C. The QPPO-based membrane water electrolyzer operated for 111 h before having a catastrophic failure/short circuit. With time, the membrane's softening results in the mesh anode's penetration into the membrane and eventually causes a short circuit with the cathode. QPPO/PTFE AEM water electrolyzer operated for 200 h at a stable performance until the experiment was terminated with no short-circuiting. Apart from the strong mechanical

strength, PTFE possesses high chemical resistance, contributing to the durability of the composite membrane. This resistance helps prevent the membrane from developing defects or undergoing chemical reactions that could lead to short-circuiting. Besides, the QPPO/PTFE composite membrane is likely to have sufficient mechanical strength to withstand the mechanical stresses and pressures associated with the water electrolyzer operation. Its structural integrity prevents the formation of cracks, pinholes, or other defects that could result in short-circuiting. In addition, the composite membrane's electrochemical stability is crucial for its prolonged operation without short-circuiting. It should be able to withstand the high voltages and current densities involved in the water electrolyzer process. The properties of QPPO and PTFE, such as their resistance to oxidation and ion transport characteristics, help maintain the necessary electrical insulation and prevent short-circuiting.

The area specific resistance (ASR) is a measure of the resistance to ionic conduction across a membrane in electrochemical devices like water electrolyzers. The ASR value indicates the membrane's ability to facilitate the efficient transport of ions during the electrochemical reaction. The QPPO-based membrane typically has an intrinsic ASR determined by its QPPO composition, while the QPPO/PTFE composite membrane's ASR is influenced by the combined properties of both QPPO and PTFE. The addition of PTFE in the composite can introduce changes in hydrophobicity and ion transport, affecting the membrane's conductivity and ASR. PTFE is known for its hydrophobic nature, which can reduce water and ion transport across the membrane. As a result, the ASR of a QPPO/PTFE composite membrane may differ from that of a QPPO-based membrane. Generally, a higher ASR is expected for a QPPO/PTFE composite membrane compared with a QPPO-based membrane due to the introduction of the less conductive PTFE component. Figure 5b–e shows the EIS and polarization curves of the QPPO-based membrane (110 μm) and QPPO/PTFE composite membrane (76 μm) before and after long-term tests. The initial ASR of the PPO-based membrane was 0.063 Ωcm^{-2}, much lower than that of the QPPO/PTFE composite membrane of 0.5 Ωcm^{-2}. After 20 and 40 h, the QPPO-based membrane impedance increased to 0.088 and 0.14 Ωcm^{-2}, respectively. The doubling of ASR after 40 h can be explained by the possible loss of IEC due to the use of 0.1 M supporting electrolytes. Thus, maintaining a low ASR is crucial for the operation and efficiency of the electrolyzer. It should be noted that supporting electrolytes mitigate losses from catalytic activity due to ionomer degradation. Given the high operating current density of QPPO, the increase in ASR results in a significant increase in IR losses and hence electrolyzer voltage to maintain the same current density at 20 and 30 h. For QPPO/PTFE composite membrane, after 200 h, the ASR also almost doubled from 0.5 to 0.9 Ωcm^{-2}. However, given the lower operating current density, the increase in IR losses has a limited effect on the polarization curve. QPPO-based membrane current at 2 V decreased from 0.95 to 0.68 Acm^{-2} and 0.59 Acm^{-2} after 20 and 40 h, respectively. For QPPO/PTFE composite membrane, the current density decreased from 0.15 to 0.135 Acm^{-2} after 40 h.

4 | CONCLUSION

Reinforced QPPO composite AEM was prepared using PTFE as the substrate. The mechanical stress significantly increased by 88%, from 16.5 to 31 MPa. The conductivity of the composite membrane is still relatively low, 11.3 $mScm^{-1}$ and 2.6%, respectively, due to the poor QPPO impregnation in PTFE pores, with only 31.4% of pores being filled. The PPO-based membrane has higher water sorption than QPPO/PTFE composite membranes, resulting in additional conductivity losses in the composite membrane. At 40% RH, the net change mass is 10.98%, while the composite membrane is 1.59%. Notably, the reinforcement strategy of AEM using PTFE composite demonstrated success with failure-free 200 h of operation, in comparison with 111 h for pristine QPPO. The results underscored the viability of reinforced membranes for enhancing cell durability. For future research, improving QPPO impregnation is essential, which could be achieved by enhancing doping solution concentration and immersion time.

AUTHOR CONTRIBUTIONS

Zhiming Feng: Conceptualization (lead); data curation (lead); formal analysis (lead); investigation (lead); methodology (lead); writing – original draft (lead). **Gaurav Gupta:** Formal analysis (supporting); methodology (supporting); supervision (supporting); writing – review and editing (supporting). **Mohamed Mamlouk:** Conceptualization (equal); formal analysis (equal); methodology (supporting); project administration (equal); resources (equal); supervision (lead); writing – review and editing (equal).

ACKNOWLEDGMENTS

We would like to acknowledge the financial support of UK Research and Innovation (UKRI)/Engineering and Physical Sciences Research Council (EPSRC) under grant number EP/T00939X/1.

CONFLICT OF INTEREST STATEMENT

No conflicts of interest exist.

DATA AVAILABILITY STATEMENT

Data will be made available on request.

ORCID

Zhiming Feng https://orcid.org/0000-0002-5882-9626

REFERENCES

[1] Z. He, G. Wang, C. Wang, L. Guo, R. Wei, G. Song, D. Pan, R. Das, N. Naik, Z. Hu, Z. Guo, *Polym. Rev.* **2021**, *61*, 689.
[2] C. Wang, Z. Feng, Y. Zhao, X. Li, W. Li, X. Xie, S. Wang, H. Hou, *Int. J. Hydrogen Energy* **2017**, *42*, 29988.
[3] X. Li, Y. Zhao, Z. Feng, X. Xiang, S. Wang, X. Xie, V. K. Ramani, *J. Membr. Sci.* **2017**, *528*, 55.
[4] I. Vincent, D. Bessarabov, *Renewable Sustainable Energy Rev.* **2018**, *81*, 1690.
[5] G. Merle, M. Wessling, K. Nijmeijer, *J. Membr. Sci.* **2011**, *377*, 1.
[6] S. Gottesfeld, D. R. Dekel, M. Page, C. Bae, Y. Yan, P. Zelenay, Y. S. Kim, *J. Power Sources* **2018**, *375*, 170.
[7] Z. Wang, J. Parrondo, V. Ramani, *J. Electrochem. Soc.* **2017**, *164*, F1216.
[8] C. G. Arges, L. Wang, J. Parrondo, V. Ramani, *J. Electrochem. Soc.* **2013**, *160*, F1258.
[9] Y. Zhao, X. Li, W. Li, Z. Wang, S. Wang, X. Xie, V. Ramani, *J. Power Sources* **2019**, *444*, 227250.
[10] Y. Yao, Y. Luo, H. Lu, B. Wang, *Compos. Struct.* **2018**, *192*, 507.
[11] J. Liu, Y. Liu, W. Yang, Q. Ren, F. Li, Z. Huang, *J. Power Sources* **2018**, *396*, 265.
[12] S. Xu, D. Lu, P. Wang, Y. Zhao, Y. Sun, J. Qi, J. Ma, *J. Membr. Sci.* **2020**, *601*, 117885.
[13] K. T. Park, S. G. Kim, J. H. Chun, D. H. Jo, B.-H. Chun, W. I. Jang, G. B. Kang, S. H. Kim, K. B. Lee, *Int. J. Hydrogen Energy* **2011**, *36*, 10891.
[14] B. Shi, J. Zhang, W. Wu, J. Wang, J. Huang, *J. Membr. Sci.* **2019**, *569*, 166.
[15] M. Qiu, B. Zhang, H. Wu, L. Cao, X. He, Y. Li, J. Li, M. Xu, Z. Jiang, *J. Membr. Sci.* **2019**, *573*, 1.
[16] Z. Feng, G. Gupta, M. Mamlouk, *Int. J. Hydrog. Energy* **2023**, *48*, 25830.
[17] N. H. Rathod, V. Yadav, A. Rajput, J. Sharma, D. K. Shukla, V. Kulshrestha, *Colloid Interface Sci. Commun.* **2020**, *36*, 100265.
[18] N. Chen, C. Long, Y. Li, D. Wang, H. Zhu, *Electrochim. Acta* **2018**, *268*, 295.
[19] Y. J. Lee, M. S. Cha, S. G. Oh, S. So, T. H. Kim, W. S. Ryoo, Y. T. Hong, J. Y. Lee, *RSC Adv.* **2019**, *9*, 27500.
[20] A. M. Ahmed Mahmoud, K. Miyatake, *ACS Appl. Energy Mater.* **2022**, *5*, 15211.
[21] H. H. Wang, C. Hu, J. H. Park, H. M. Kim, N. Y. Kang, J. Y. Bae, W. H. Lee, N. Chen, Y. M. Lee, *J. Membr. Sci.* **2022**, *644*, 120160.
[22] C.-K. Hwang, K. A. Lee, J. Lee, Y. Kim, H. Ahn, W. Hwang, B.-K. Ju, J. Y. Kim, S. Y. Yeo, J. Choi, Y.-E. Sung, I.-D. Kim, K. R. Yoon, *Nano Energy* **2022**, *101*, 107581.
[23] F. Zhang, H. Zhang, J. Ren, C. Qu, *J. Mater. Chem.* **2010**, *20*, 8139.
[24] Y. Zhao, H. Yu, D. Xing, W. Lu, Z. Shao, B. Yi, *J. Membr. Sci.* **2012**, *421-422*, 311.
[25] T. S. Mayadevi, K. Min, O. Choi, J. E. Chae, H.-J. Kim, C. H. Choi, H. Kang, C. H. Park, T.-H. Kim, *Int. J. Hydrogen Energy* **2022**, *47*, 16222.
[26] D. Zhang, S. Xu, R. Wan, Y. Yang, R. He, *J. Power Sources* **2022**, *517*, 230720.
[27] Z. Feng, G. Gupta, M. Mamlouk, *RSC Adv.* **2023**, *13*, 20235.
[28] S. Sung, T. S. Mayadevi, K. Min, J. Lee, J. E. Chae, T.-H. Kim, *J. Membr. Sci.* **2021**, *619*, 118774.
[29] Z. Feng, P. O. Esteban, G. Gupta, D. A. Fulton, M. Mamlouk, *Int. J. Hydrogen Energy* **2021**, *46*, 37137.
[30] G. Gupta, K. Scott, M. Mamlouk, *J. Power Sources* **2018**, *375*, 387.
[31] R. Espiritu, B. T. Golding, K. Scott, M. Mamlouk, *J. Mater. Chem. A* **2017**, *5*, 1248.
[32] P. Knauth, L. Pasquini, R. Narducci, E. Sgreccia, R. A. Becerra-Arciniegas, M. L. Di Vona, *J. Membr. Sci.* **2021**, *617*, 118622.
[33] M. T. Q. S. da Silva, M. do Rocio Cardoso, C. M. P. Veronese, W. Mazer, *Mater. Today: Proc.* **2022**, *58*, 1344.
[34] S. Adnan, M. Hoang, H. Wang, Z. Xie, *Desalination* **2012**, *284*, 297.
[35] B. Tjaden, S. J. Cooper, D. J. L. Brett, D. Kramer, P. R. Shearing, *Curr. Opin. Chem. Eng.* **2016**, *12*, 44.
[36] H. T. Hamad, D. W. Abbood, A. S. Mustafa, *IOP Conf. Ser.: Mater. Sci. Eng.* **2018**, *454*, 012093.
[37] G. Madabattula, S. Kumar, *J. Electrochem. Soc.* **2020**, *167*, 080535.
[38] S. J. Cooper, A. Bertei, P. R. Shearing, J. A. Kilner, N. P. Brandon, *SoftwareX* **2016**, *5*, 203.
[39] M. A. Al-Ghouti, D. A. Da'ana, *J. Hazard. Mater.* **2020**, *393*, 122383.

How to cite this article: Z. Feng, G. Gupta, M. Mamlouk, *J. Appl. Polym. Sci.* **2024**, e55340. https://doi.org/10.1002/app.55340